Biochemical Pharmacology, Vol. 44, No. 7, pp. 1417–1429, 1992.
Printed in Great Britain.

0006-2952/92 $5.00 + 0.00

BINDING OF 2-ACETYLPYRIDINE-5-[(2-CHLOROANILINO)THIOCARBONYL] THIOCARBONOHYDRAZONE (BW348U87) TO HUMAN SERUM ALBUMIN

DAVID J. T. PORTER*
Experimental Therapy Division, Wellcome Research Laboratories, Research Triangle Park, NC 27709, U.S.A.

(*Received* 25 *February* 1992; *accepted* 5 *June* 1992)

Abstract—Dissociation constants and rate constants for the binding of 2-acetylpyridine-5-[(2-chloroanilino)thiocarbonyl]thiocarbonohydrazone (**I**, BW348U87), an agent that enhances the antiherpetic efficacy of acyclovir, to human serum albumin have been determined. **I** quenched the fluorescence of human serum albumin, whereas the absorbance of **I** at 370 nm increased upon binding to the protein. The absorbance change was attributed to preferential binding of anionic **I** (pK_a 7.0). Titration data indicated multiple binding sites for **I**. The dissociation constant of the high-affinity site was 0.11 μM. The time course for binding of **I** to 100 nM human serum albumin was biphasic. The early and late phases were described by first-order rate constants that had maximal values of 100 and 11 sec^{-1}, respectively. The rate constant for the dissociation of **I** from human serum albumin was estimated to be 6 sec^{-1}. Dodecyl sulfate and octanoate displaced **I** from human serum albumin·**I** with rate constants of 4.5 and 7.3 sec^{-1}, respectively. Since the fluorescence emission spectrum of human serum albumin and the absorption spectrum of **I** overlapped significantly (the spectral overlap integral, J, was 2.6×10^{-14} M^{-1} cm^3), the possibility of Förster dipole-dipole energy transfer was considered. However, a significant fraction of the fluorescence quenching by **I** resulted from a conformational change in the protein upon binding of **I** and was not the result of dipole-dipole energy transfer. Nonetheless, the distance between one of the binding regions for **I** on human serum albumin and a tryptophan residue in the protein was estimated to be 31 Å by this method. The high affinity of **I** for albumin could be related to its low hematological toxicity.

Thiocarbonohydrazones potentiate the *in vitro* antiherpetic action of acyclovir against herpes simplex virus 1, herpes simplex virus 2, and varicella-zoster virus [1, 2]. The mechanism for this synergy is partially explained by the time-dependent "inactivation" of viral ribonucleotide reductases [2–4]. Thus, inactivation of these enzymes decreases cellular 5′-deoxyguanosine triphosphate concentration such that acyclovir triphosphate is incorporated more frequently into the viral DNA. Surprisingly, thiocarbonohydrazones also cause a 9-fold elevation of cellular acyclovir triphosphate concentration that further enhances the frequency at which acyclovir triphosphate is incorporated into viral DNA [2]. Consequently, thiocarbonohydrazones and acyclovir are synergistically therapeutic reagents for the topical treatment of HSV-infected animal models [1, 5, 6]. The dimethylthiocarbonohydrazone derivative (**II**) (see Structure 1) was selected initially for development, but subsequently was found to have hematological toxicity at high oral doses in rats [1]. The 2-chloroanilino analogue, 2-acetylpyridine-5-[(2-chloroanilino)thiocarbonyl]thiocarbonohydrazone (**I**, BW348U87), however, has a satisfactory toxicity profile and is currently being developed in combination with acyclovir as a topical antiherpetic agent [1].

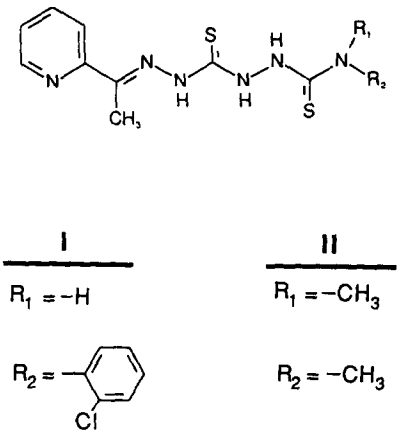

Structure 1.

The binding of drugs to blood proteins affects their therapeutic, pharmacodynamic, and toxicological actions [7]. Furthermore, drug binding to albumin can affect the toxicity of endogenous substances. For example, the toxicity of bilirubin is decreased by binding to human serum albumin (HSA)†, but

* Correspondence: Dr. David J. T. Porter, Experimental Therapy Division, Wellcome Research Laboratories, 3030 Cornwallis Road, Research Triangle Park, NC 27709. Tel. (919) 248-8699; FAX (919) 248-8747.

† Abbreviations: HSA, human serum albumin; and SDS, sodium dodecyl sulfate.

certain drugs such as sulfonamides and bucolome can displace bilirubin from albumin to cause fatal kernicterus or brain damage [8, 9]. Even though **I** is being developed as a tropical treatment for HSV infections, it was relevant to investigate the binding of **I** and **II** to serum albumin. For instance, the differential hematological toxicology for orally administered **I** and **II** [1] could be related to the differential binding of these analogues to serum albumin. We have investigated by spectroscopic techniques the kinetics and thermodynamics for the binding of **I** to human serum albumin. In summary, we found multiple binding sites for compound **I** on human serum albumin. The site with the highest affinity for **I** had a dissociation constant of 0.11 μM. In contrast, human serum albumin bound **II** weakly with a dissociation constant of 340 μM.

EXPERIMENTAL PROCEDURES

Materials

Essentially fatty acid-free (<0.005%) HSA (A-1887) was purchased from the Sigma Chemical Co. (St. Louis, MO). Lot numbers 119F9303 and 118F9311 were used in these studies and are referred to as Lot 1 and Lot 2, respectively. These preparations were homogeneous on sodium dodecyl sulfate (SDS) polyacrylamide gel (10%) electrophoresis. Since more than 80% of albumin is in the monomeric form and the binding properties of monomeric and dimeric protein are similar [10], the protein was not fractionated into monomeric and dimeric forms. Sodium octanoate, ibuprofen, 3-(α-acetonylbenzyl)-4-hydroxycoumarin (warfarin), bilirubin, and sodium salicylate were purchased from the Sigma Chemical Co. **I**, **II**, and 2-acetylpyridine thiocarbonohydrazide (**III**) were synthesized as reported previously [11]. 4-(2-Chlorophenyl)thiosemicarbazide (**IV**) was purchased from Trans-World Chemicals, Inc. (Rockville, MD).

General methods

Human serum albumin was dissolved in the standard buffer (50 mM sodium or potassium phosphate and 1 mM EDTA at pH 7.0) and the concentration was determined spectrophotometrically with an $\varepsilon_{278} = 39{,}800\ M^{-1}\,cm^{-1}$ [12]. Saturated solutions of **I**, **II**, and **III** were prepared by sonication of excess compound in 2 mM NaOH for 5 min. The mixture was filtered through a 0.22 μm filter and the concentration of the analogue in solution was determined spectrophotometrically. The extinction coefficients in the standard buffer were: **I**, $\varepsilon_{310} = 25\ mM^{-1}\ cm^{-1}$; **II**, $\varepsilon_{310} = 25\ mM^{-1}\ cm^{-1}$; and **III** $\varepsilon_{305} = 20.5\ mM^{-1}\ cm^{-1}$. Bilirubin was dissolved in 5 mM NaOH and the concentration was measured by the absorbance at 440 nm and an $\varepsilon_{440} = 47.5\ mM^{-1}\ cm^{-1}$ [13]. Solutions of sodium dodecyl sulfate, sodium salicylate, ibuprofen sodium octanoate, warfarin, and **IV** were prepared gravimetrically. The standard buffer was prepared with potassium phosphate for all measurements except for those involving dodecyl sulfate. In this case the standard buffer was prepared with sodium phosphate.

In some titration experiments, the concentration of **I** was increased to 50 μM, which was greater than its solubility (~10 μM). Since the absorbance of **I** at 310 nm in these supersaturated solutions was stable over the course of the titration, **I** was not precipitating out of solution during the experiment (<30 min).

Acquisition of spectral data

Optical spectral data were collected on a UVIKON 860 spectrophotometer (Kontron, Everret, MA) and fluorescence spectra were recorded on a Kontron SFM 25 spectrofluorometer. The fluorescence emission of HSA was usually monitored at 340 nm with an excitation wavelength of 280 nm. The excitation wavelength was increased to 300 nm when only tryptophanyl residues were excited. Fluorescence data were corrected for inner and outer filter effects by the factor $\exp(2.303 \cdot A)$, where A was the average absorbance at the excitation and emission wavelength. Experimental conditions were chosen such that these corrections amounted to no more than 15% of the total signal. Rapid kinetic data were collected with a SF.17MV Stopped-flow Spectrofluorimeter (Applied Photophysics Limited, Leatherhead, U.K.). The time-constant for the instrument was less than one-tenth of the fastest relaxation time monitored. The entrance and exit slits were 2 mm. Other parameters were adjusted as described in the manual from the manufacturer. Fluorescence (scattering) data were collected with an excitation wavelength of 280 nm. The path length for the excitation beam was 2 mm and the path length for emission was 10 mm. Absorbance data were collected with a 10-mm path length. All reactions were initiated by mixing equal volumes of reactants. Five or more experiments were averaged.

Titration of human serum albumin. The moles of thiocarbonohydrazone derivative bound per mole of HSA were determined as a function of free thiocarbonohydrazone concentration (L). The stoichiometric binding equation [14, 15] was fitted to these data. It was found that an equation with three stoichiometric dissociation constants (equation 1) fitted the titration data well.

$$r = \frac{(K_1)^{-1}[L] + 2\cdot(K_1\cdot K_2)^{-1} + 3\cdot(K_1\cdot K_2\cdot K_3)^{-1}[L]^3}{1 + (K_1)^{-1}[L] + (K_1\cdot K_2)^{-1}[L]^2 + (K_1\cdot K_2\cdot K_3)^{-1}[L]^3} \quad (1)$$

where K_1, K_2, and K_3 were the stoichiometric dissociation constants for binding of the first, second, and third molecule of L to HSA, respectively.

The fluorescence changes of HSA (excitation 280 nm, emission 340 nm) associated with ligand binding were used to monitor the titration of HSA by ligand. Dissociation constants for tight binding and loose binding sites were calculated from these data as follows. When the dissociation constant of the titrant was much greater than the concentration of HSA, it was valid to assume that the concentration of free ligand was equal to the concentration of added ligand (L_t). Thus, it was appropriate to fit equation 2a to these titration data to yield the fractional fluorescence decrease (relative to free HSA) upon complex formation (A) and the dissociation constant (K_{d1}). When the dissociation constant of the ligand was similar to the concentration of HSA, analysis of the titration data was more

complicated. In this case, the concentration of free ligand was not approximated by L_t. It was necessary to calculate the fractional saturation of the tight binding site (f) from the solution to a quadratic equation (equation 2b) that related L_t, K_{d2} and the concentration of tight binding sites (A_t). Thus, equation 2c was fitted to data for titration of a single tight binding site with a dissociation constant of K_{d2} and with a fractional fluorescence decrease of B upon complex formation. When a tight binding site and a loose binding site for ligand were present on HSA, equation 2d was fitted to the titration data. Equation 2d was the sum of equation 2a and equation 2c. This equation assumed that K_{d1} was much greater than A_t so that L_t was a reasonable approximation to free ligand during the titration of the site with the larger dissociation constant.

$$\text{Fractional fluorescence} = 1 + A \cdot \frac{[L_t]}{K_{d1} + [L_t]} \quad (2a)$$

$$f = 1/2 \cdot \frac{(A_t + L_t + K_{d2})}{A_t} - 1/2 \cdot \left(\left(\frac{A_t + L_t + K_{d2}}{A_t} \right)^2 - 4 \frac{L_t}{A_t} \right)^{1/2} \quad (2b)$$

$$\text{Fractional fluorescence} = 1 + B \cdot f \quad (2c)$$

$$\text{Fractional fluorescence} = 1 + B \cdot f + A \cdot \frac{[L_t]}{K_{d1} + [L_t]} \quad (2d)$$

A typical titration was made with 20–30 concentrations of titrant.

Time courses for quenching of HSA fluorescence. Single and double exponential functions were fitted to the time courses for fluorescence quenching of HSA by a ligand (400 data points) to obtain pseudo first-order rate constants for binding of the ligand to HSA. The software for these fitting routines was provided with the SF.17MV Stopped-flow Spectrofluorimeter. If the observed rate constants (K_{obs}) were linearly dependent on the concentration of ligand, equation 3a was fitted to the data; k_s was the slope of a linear plot of k_{obs} versus $[L]$. If the observed rate constants approached a limiting value at high concentrations of ligand and extrapolated to zero at zero concentrations of ligand, equation 3b was fitted to the data. The apparent dissociation constant was K_a and the limiting value of the first-order rate constant was k. If the value of the observed rate constant had a limiting value at high concentrations of ligand, but did not extrapolate to zero at zero concentration of ligand, equation 3c was fitted to the data. The apparent dissociation constant was K_a and the nonzero intercept at zero ligand concentration was k_0. The limiting value of the first-order rate constant at high ligand concentrations was k.

$$k_{obs} = k_0 + k_s[L] \quad (3a)$$

$$k_{obs} = \frac{k[L]}{K_a + [L]} \quad (3b)$$

$$k_{obs} = \frac{(k - k_0)[L]}{[L] + K_a} + k_0 \quad (3c)$$

The constants defined by these equations were estimated by the iterative nonlinear least squares fitting routine outlined by Bevington [16].

Calculation of distance between I and tryptophan in HSA·I

Since the emission spectrum of HSA and the absorption spectrum of I overlap (see Results), quenching of protein fluorescence by the Förster dipole-dipole excitation transfer mechanism, such as that described for the binding of HSA to bilirubin or *cis*-parinaric acid [17], was possible. The equations used for these calculations were taken from Stryer [18]. The distance (R_0) between the donor and acceptor that produces 50% fluorescence quenching was calculated by equation 4 where Q_0 was the quantum yield of the tryptophan acceptor, κ^2 was the orientation factor, and N was the refractive index [18]. Berde *et al.* [17] determined values for Q_0 and N for HSA of 0.3 and 1.45, respectively. The orientation factor κ^2 was assumed to be 2/3 (see Stryer for a discussion of the uncertainty this assumption introduces into the calculation [18]). The spectral overlap integral (J) between the absorption spectrum of I and the emission spectrum of HSA was given by equation 5.

$$R_0 = (J\kappa^2 Q_0 N^{-4})^{1/6} \times 9.7 \times 10^3 \text{ Å} \quad (4)$$

$$J = \frac{\int F(\lambda)\varepsilon(\lambda)\lambda^4 d\lambda}{\int F(\lambda) d\lambda} \text{ M}^{-1} \text{ cm}^3 \quad (5)$$

where F is a relative fluorescence. The efficiency for quenching (E) was calculated by equation 6

$$E = \frac{Q_0 - Q_t}{Q_0} \quad (6)$$

where Q_0 was the relative fluorescence yield of HSA·I in the absence of fluorescence energy transfer and Q_t was the relative fluorescence yield of HSA·I in the presence of fluorescence energy transfer. The distance (r) between tryptophan and the binding region for I was calculated from the values of E and R_0 by equation 7.

$$E = \frac{r^{-6}}{r^{-6} + R_0^{-6}} \quad (7)$$

RESULTS

Perturbations of the spectral properties of I and HSA

HSA perturbed the optical spectrum of I. The changes were similar to those that occurred upon increasing the pH of a solution of I from pH 7 to pH 12 in the absence of HSA (Fig. 1A). The pK_a values for I were determined by spectrophotometric titration at 350 nm to be 7.0 ± 0.1 and 3.9 ± 0.1 (data not shown). These results suggested that human serum albumin preferentially bound the anionic form of I.

The difference spectra between free I and I bound to 10 μM HSA with ratios of albumin to I of 2 and 0.4 were superimposable after normalization to the

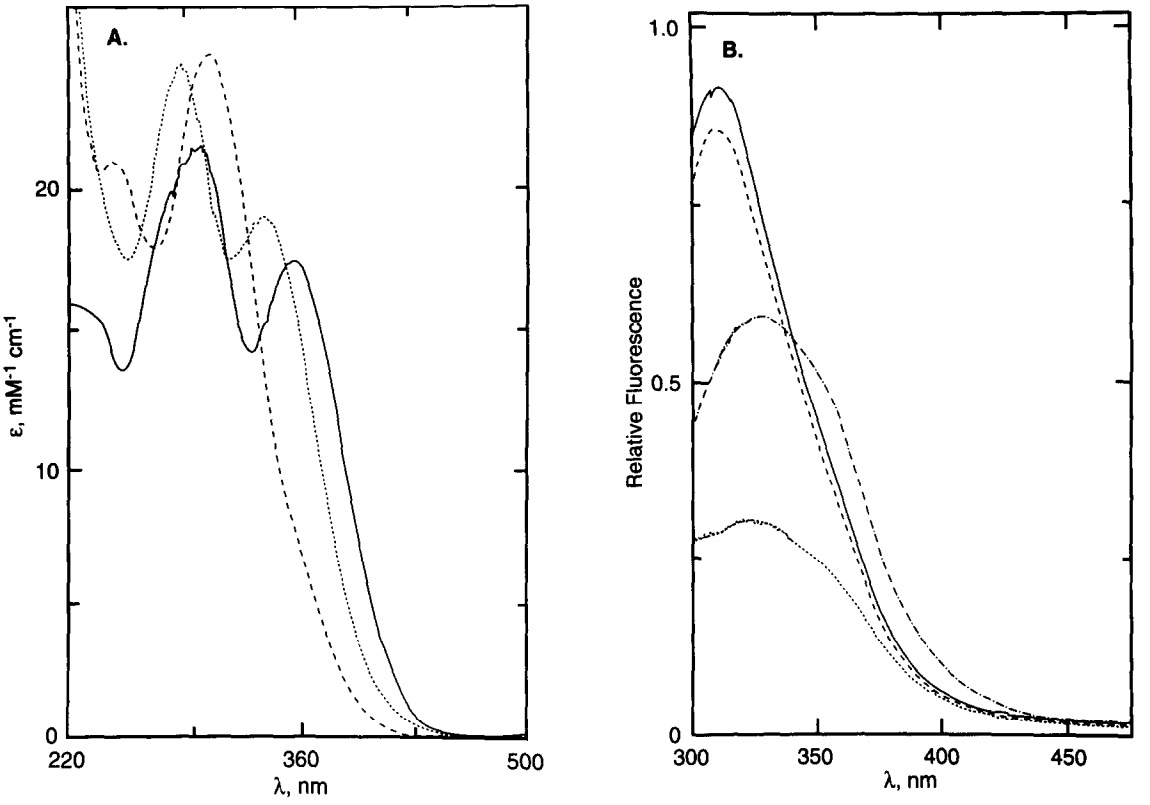

Fig. 1. Optical and fluorescence changes associated with the binding of I and/or dodecyl sulfate to HSA. (A) Optical spectra of I at pH 7.0 (---), at pH 12 (• • • •) and at pH 7.0 in the presence of 10 μM HSA (—). The concentration of I was 5 μM. (B) Effect of I and dodecyl sulfate on the fluorescence emission spectra of 0.1 μM HSA (280 nm excitation wavelength) in the standard buffer. The fluorescence of HSA (-•-) was quenched by 1 μM I (• • • •), but was enhanced by 200 μM dodecyl sulfate (—). The fluorescence emission spectrum of the HSA·I complex (2 μM I) was converted to that of the HSA·dodecyl sulfate complex by addition of 200 μM dodecyl sulfate to HSA·I (---).

peak absorbance value at 370 nm. Thus, the increase in absorbance at 370 nm was proportional to the concentration of HSA·I. Addition of a substoichiometric amount of I to HSA yielded an absorbance increase at 370 nm that corresponded to a $\Delta\varepsilon_{370} = 14\ mM^{-1}\ cm^{-1}$.

Alternatively, the fluorescence of HSA was quenched upon binding of I. This effect was reversed by dodecyl sulfate (Fig. 1B).

Dissociation constants of HSA for I

The dissociation constants of HSA for I were calculated from titration data in which the absorbance change at 370 nm was monitored. The concentration of the HSA·I complex was calculated from the absorbance increase at 370 nm. The concentration of free I was calculated as the difference between the total concentration of I and the concentration of the HSA·I complex. Thus, the number of molecules of I bound per mol of HSA (r) was calculated as a function of the concentration of free I (Fig. 2). Since approximately 3 mol of I were bound per mol of HSA, stoichiometric binding equation for 3 sites (equation 1) was fitted to these data to yield dissociation constants of 0.08 ± 0.04, 3.9 ± 0.8 and 30 ± 8 μM. The site with the lowest affinity (30 μM) was not considered further.

The dissociation constants of HSA for I were also determined from protein fluorescence quenching data collected with an excitation wavelength of 280 nm. The biphasic titration of protein fluorescence by I suggested that there were at least two binding sites for I (Fig. 3). Equation 2b was fitted to these data with dissociation constants of 0.11 ± 0.01 and 5 ± 3 μM. Because the inner and outer filter corrections became significant (>15%) at concentrations of I greater than 5 μM, the titration data were only collected from 0 to 5 μM I. Consequently, the larger dissociation constant had considerable error associated with it. Nonetheless, these dissociation constants were similar to the two smaller dissociation constants determined from the above titration data in which the absorbance change at 370 nm was monitored.

HSA was also titrated spectrofluorometrically with I at pH 8.0 in 0.1 M potassium phosphate and 1 mM EDTA. The dissociation constants were lower at pH 8.0 (0.027 ± 0.007 and 0.6 ± 0.09 μM) compared

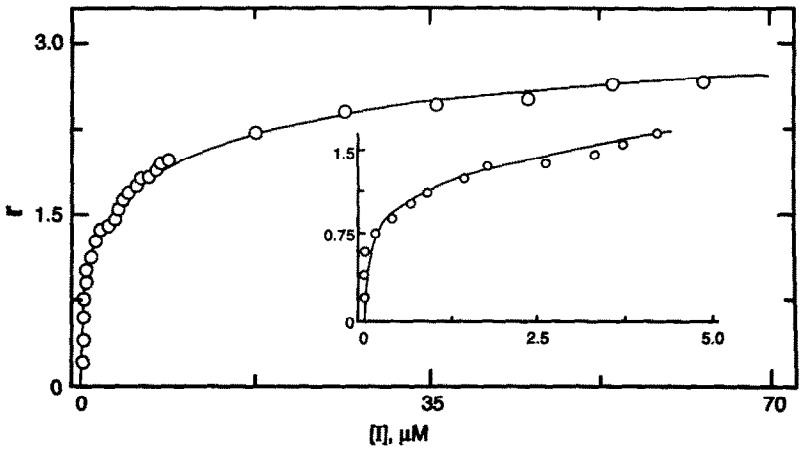

Fig. 2. Stoichiometric binding of I to HSA. HSA (10 μM) was titrated with I in the standard buffer. The concentration of I bound to HSA was calculated from the absorbance increase at 370 nm and a $\Delta\varepsilon_{370} = 14\ mM^{-1}\ cm^{-1}$. The concentration of free I was calculated as the difference between the total concentration of I and the concentration of bound I. The initial portion of this titration is presented in the inset. The solid line was calculated from the fit of equation 1 to these data.

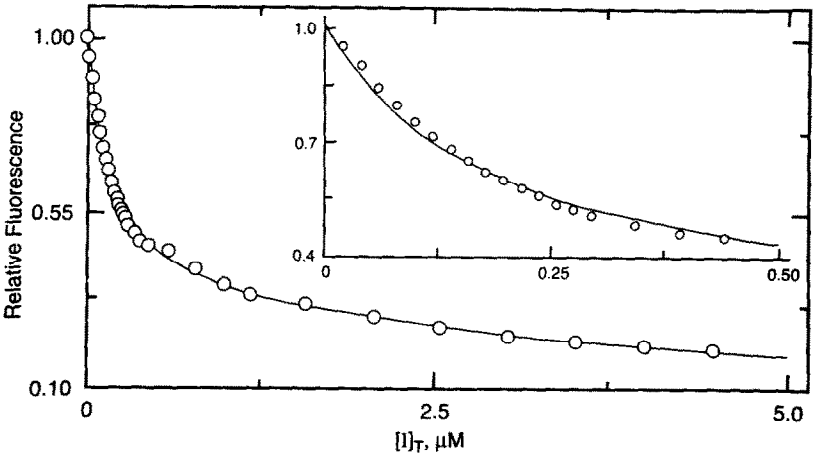

Fig. 3. Spectrofluorometric titration of HSA with I in the standard buffer. The relative fluorescence of 65 nM HSA was measured as a function of the total concentration of I (I_t). At the highest concentration of I a 15% inner and outer filter correction was applied. The initial portion of this titration is presented in the inset. The solid line was calculated from a fit of equation 2b to these data.

to pH 7.0. Since the concentration of anionic I would increase 2-fold ($pK_a = 7$) when the pH of the medium is increased from 7 to 8, the decrease in the value of these dissociation constants with increasing pH was consistent with the anionic form of I binding to HSA.*

* The dissociation constants of HSA for I determined by spectral techniques could not be confirmed by equilibrium dialysis in the apparatus described by Reinard and Jacobsen [19], because recovery of compound I from dialysis chambers was less than 60% after a 5-hr dialysis at 25°. Similarly, the recovery of I was less than 80% after ultrafiltration of a 500 μM solution of I at pH 7.0 through a Centrifree ultrafiltration apparatus.

Association rate constant for compound I

Stopped-flow spectrofluorometry was required to monitor the time course for the binding of I to HSA. The time course for the binding of I was measured fluorometrically and was analyzed as a double exponential function (Fig. 4A). The amplitudes for the two phases of the reaction at each concentration of I were approximately equal. Furthermore, the amplitude of the fluorescence increase at pH 7.0 was less than 2-fold as the concentration of I was increased from 0.2 to 5 μM I. This was consistent with the value of a smaller dissociation constant of HSA for I (0.11 μM).

The concentration dependence of the pseudo first-

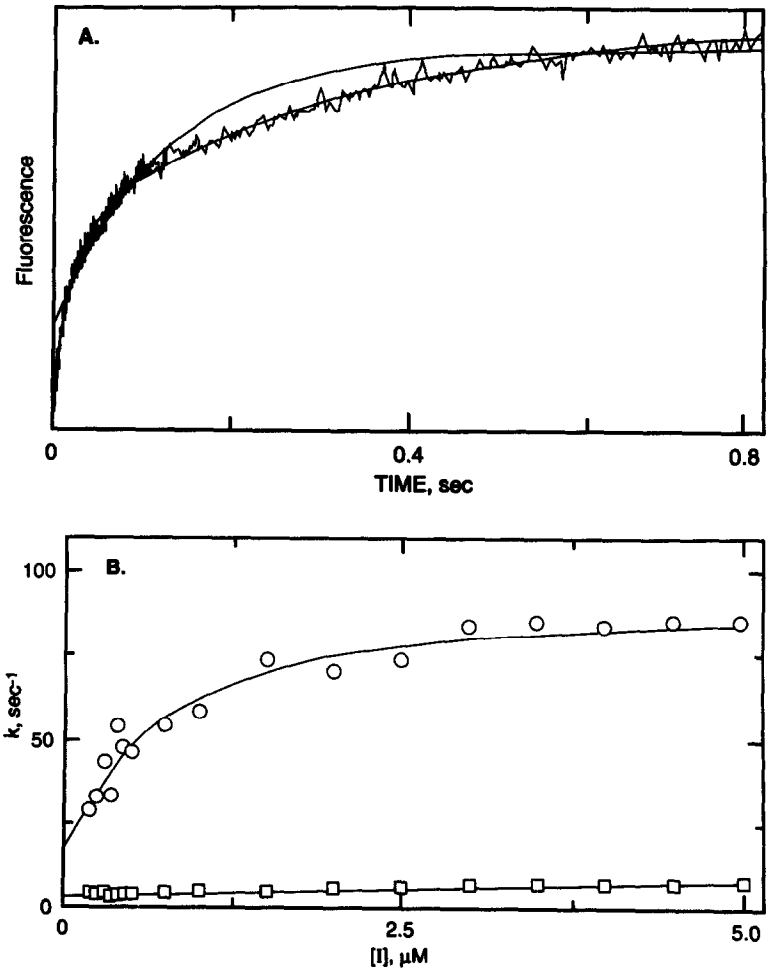

Fig. 4. Kinetics for the binding of I to HSA. The time courses for the binding of I to 50 nM HSA were monitored on the stopped-flow spectrofluorometer with an excitation wavelength of 280 nm. (A) Typical time course for reaction of HSA with 500 nM I. A double exponential function fitted the data well. The best fit of a single exponential function to the data is included to demonstrate the poor fit of this function to the data. (B) The dependence of the pseudo first-order rate constants for the two phases of the reaction on the concentration of I. The solid line was calculated from a fit of equation 3c to these data.

order rate constants for the early phase of the reaction suggested that a limiting first-order rate constant was approached at high concentrations of I (Fig. 4B). Furthermore, the nonzero value for the dissociation constant for the reaction required that k_{obs} extrapolate to a nonzero ordinate intercept (dissociation rate constant). Thus, equation 3c was fitted to these data with $k_0 = 15 \pm 9\,sec^{-1}$, $K_a = 0.8 \pm 0.3\,\mu M$, and $k = 100 \pm 10\,sec^{-1}$. Equation 3c was also fitted to the data for the late phase of the reaction $k_0 = 2.7 \pm 0.2\,sec^{-1}$, $K_a = 5 \pm 3\,\mu M$, and $k = 11 \pm 3\,sec^{-1}$. A similar set of kinetic data for the binding of I to 150 nM HSA was collected at pH 8.0. Equation 3c was fitted to the data for the early phase of the reaction with $k_0 = 16 \pm 8\,sec^{-1}$, $K_a = 0.9 \pm 0.2\,\mu M$, and $k = 220 \pm 10\,sec^{-1}$. Equation 3c was also fitted to the pseudo first-order rate constants for the late phase of the reaction with $k_0 = 4 \pm 1\,sec^{-1}$, $K_a = 1.8 \pm 0.5\,\mu M$, and $k = 26 \pm 2\,sec^{-1}$.

The biphasic time courses for binding of 20 μM I with 5 μM HSA were similar when measured by fluorescence quenching at 340 nm or by the increase in absorption at 370 nm. However, the time course for the reaction of 5 μM I with HSA was dependent on HSA concentration. The pseudo first-order rate constant for the fast phase of the reaction increased from $67\,sec^{-1}$ to $180\,sec^{-1}$ as the concentration of HSA was increased from 50 to 500 nM. The reason for the increase in this rate constant as the concentration of HSA increased was not clear. However, the rate constant was relatively independent of HSA concentration between 50 and 100 nM ($67–78\,sec^{-1}$). Kinetic measurements were made with HSA in this concentration range.

The kinetics for the binding of I to HSA were also

monitored by the absorbance changes at 370 nm (Fig. 1A). Because the absorbance changes were relatively small, a higher concentration of HSA was required for these experiments than that used for the fluorescence experiments. Thus, 20 μM I bound to 5 μM HSA in a biphasic reaction with pseudo first-order rate constants of 201 ± 4 and 16.4 ± 0.5 sec^{-1}. The ratio of the amplitudes for the early to the late phase of the reaction was 3.5. The analogous constants determined from monitoring the fluorescence changes at this concentration of HSA were 232 ± 4 and 18.8 ± 0.6 sec^{-1} with a ratio of amplitudes equal to 5.3. Since the results from the two methods were similar, the absorbance and fluorescence changes were monitoring the same processes. However, the rate constants for binding at 5 μM HSA were approximately 2-fold larger than those determined at low concentrations of HSA. This result suggested that protein–protein interactions, such as dimerization, affected the kinetics of binding of I to HSA at these protein concentrations.

First-order rate constant for the dissociation of I from HSA

The rate constant for the dissociation of I from the primary complex between HSA and I at pH 7.0 was estimated from the data of the previous section to be 15 ± 9 sec^{-1} (k_0). An alternative method for estimating the overall first-order dissociation rate constant for I was to measure the first-order rate constant for equilibration of HSA·I with HSA and I as a function of the equilibrium concentration of these species. Thus, different equilibrium mixtures of HSA, HSA·I, and I were diluted 2-fold and the rate constant for equilibration of these species to a new equilibrium state was determined. Since a single exponential function accurately fitted these relaxation data (Fig. 5), these data were analyzed in terms of a scheme (equation 8) in which I associated with HSA in a bimolecular process (k_{on}) and dissociated from HSA·I in a first-order process (k_{off}). The expression for the rate constant for equilibration (k) of these species was

$$k = k_{off} + k_{on}([HSA] + [I]) \qquad (8)$$

where the ([HSA] + [I]) was the sum of the equilibrium constants of HSA and I [20]. The value for k_{off} was 5.7 ± 0.9 sec^{-1}* and the value for k_{on} was 2.6×10^7 M^{-1} sec^{-1}. The dissociation constant calculated from these values was 0.22 μM, which was similar to the measured value for the smaller dissociation constant (0.11 μM).

* An alternative method for determining the dissociation rate constant for I and HSA was to trap I as it was released from HSA. Since I was complexed tightly by Fe^{2+} [3], it was possible that the rate of release of I from HSA·I could be determined by addition of Fe^{2+} to HSA·I. However, the rate constant for the reaction of 20 μM $FeSO_4$ with 6 μM I was only 4.42 ± 0.01 sec^{-1} (data not shown), which was too small to make ferrous sulfate an effective trap for I. Alternatively, I was found to be oxidized by horse radish peroxidase. The first-order rate constant for the oxidation of 2.5 μM I by 0.5 μM peroxidase and 50 μM H_2O_2 was 0.15 ± 0.01 sec^{-1} (data not shown). This trapping reaction was also too slow to be used for determination of the dissociation rate constant for I and HSA.

Displacement of I from HSA·I by dodecyl sulfate and octanoate

I quenched the fluorescence of HSA, whereas dodecyl sulfate enhanced the fluorescence of HSA (Fig. 1B). The fluorescence of the HSA·I complex was enhanced by dodecyl sulfate to a level that was comparable to the fluorescence of the HSA–dodecyl sulfate complex (Fig. 1B). Furthermore, dodecyl sulfate reversed the absorbance changes associated with binding of I to 10 μM HSA (Fig. 6). These results suggested that dodecyl sulfate displaced I from the HSA·I complex. Fluorescence titration studies of HSA with dodecyl sulfate indicated that there are multiple tight binding sites on HSA for dodecyl sulfate and that the fluorescence of the protein is enhanced only after approximately 3 mol of dodecyl sulfate are bound per mol of HSA [21]. Thus, equation 2a did not fit the titration data for displacement of I from HSA by dodecyl sulfate at high concentrations of HSA (Fig. 6). Nonetheless, the decrease in the absorbance of I bound to HSA correlated with the increase in HSA fluorescence.

Octanoate, which binds specifically to the indole and benzodiazepine-binding site on human serum albumin [12, 22], also displaced I from the protein (data not shown).

Kinetics for dissociation of I from HSA·I in the presence of dodecyl sulfate and octanoate

The kinetics for displacement of I from HSA·I by dodecyl sulfate were similar when monitored by the fluorescence increase or by the absorbance decrease at 370 nm that were associated with displacement of I from HSA·I. The displacement reaction was first-order in HSA·I and the pseudo first-order rate constant increased with increasing concentrations of dodecyl sulfate (Fig. 7). The first-order rate constant for dissociation of I from HSA·I at low concentrations of dodecyl sulfate was 6.0 ± 0.7 sec^{-1} (Fig. 7), which was similar to the rate constant for the dissociation of I from HSA·I of 5.7 ± 0.9 sec^{-1} estimated from the data of Fig. 5. These results suggested that dodecyl sulfate displaced I from HSA·I by competing for the same binding site. However, the binding data (Fig. 6) indicated that several mol of dodecyl sulfate bound per mol of HSA·I prior to displacement of I. Thus, even though displacement of I from HSA·I was not a simple competition reaction, the effects on the I binding site that resulted from the binding of dodecyl sulfate to other sites on the albumin molecule did not have a large effect on the rate constant for dissociation of I from HSA·I. The secondary effects of dodecyl sulfate binding could account for the increase in the rate constant for dissociation of I at increasing concentrations of dodecyl sulfate.

The rate constant for dissociation of I from HSA·I was estimated from the kinetics for displacement of I from HSA·I by octanoate. There was little fluorescence change of HSA upon addition of octanoate, but octanoate converted the fluorescence spectrum of HSA·I to that characteristic of HSA (data not shown). These results suggested that octanoate displaced I from HSA·I. Octanoate reacted with HSA·I in a first-order process that was

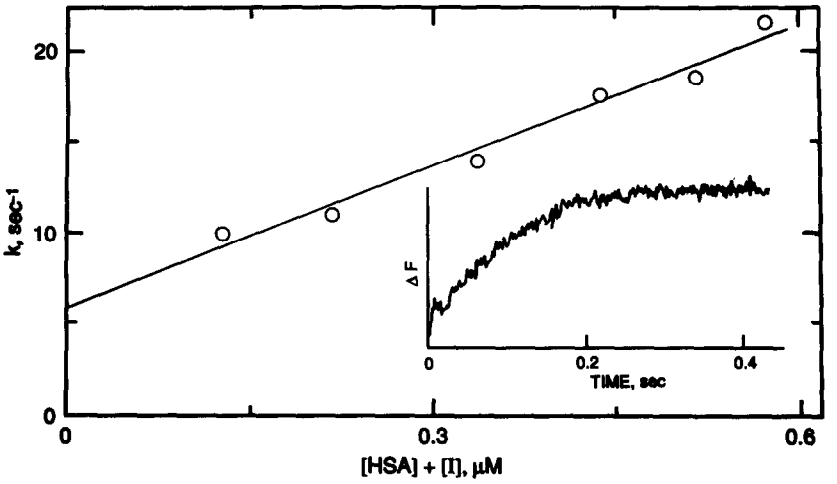

Fig. 5. Rate constant for dissociation of I from HSA·I. Dissociation of I from HSA·I was followed by the fluorescence increase (excitation wavelength of 280 nm) due to formation of free HSA upon a 2-fold dilution of a solution of the HSA·I complex. A typical time course for the fluorescence increase upon a 2-fold dilution of HSA·I that was formed from 0.2 μM I and 0.2 μM HSA is presented in the inset. The dependence of the pseudo first-order rate constant for the approach to equilibrium was measured as a function of the sum of the equilibrium concentrations of HSA and I ([HSA] + [I]). The equilibrium concentrations of I and HSA were calculated from the total concentrations of HSA and I and the high-affinity dissociation constant of 0.11 μM. The solid line was calculated from a fit of equation 3a to these data.

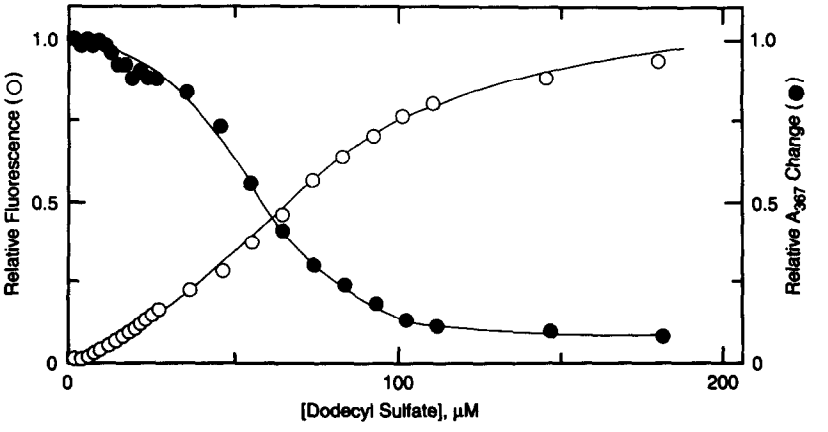

Fig. 6. Displacement of I from HSA·I by dodecyl sulfate. The release of I from HSA·I (10 μM HSA and 5 μM I) was monitored either by the absorbance decrease at 367 nm or by the fluorescence increase at 315 nm (excitation wavelength of 280 nm). The relative changes in absorbance and fluorescence were measured as a function of the total dodecyl sulfate concentration.

dependent on octanoate concentration (data not shown). The concentration dependence for the displacement reaction was similar to that observed with dodecyl sulfate. The dissociation rate constant at low concentrations of octanoate was 7.3 ± 0.5 sec^{-1}, which was similar to the value observed with dodecyl sulfate (4.5 ± 0.7 sec^{-1}). The pseudo first-order rate constant increased with octanoate concentration with a value of (1.3 ± 0.08) × 10^3 M^{-1} sec^{-1} compared to the value of (4.5 ± 0.3) × 10^5 M^{-1} sec^{-1} for dodecyl sulfate. The increase in the rate constant for dissociation of I from HSA·I as the concentration of octanoate increased was similar to the effect observed with dodecyl sulfate and was probably due to multiple binding regions on HSA for octanoate.

Effect of ligands on the pseudo first-order rate constants for the binding of I by HSA

Kragh-Hansen defined six regions on HSA that bind specific ligands with high affinity [8]. Long-chain fatty acids bind to site 1 with high affinity, octanoate binds site 2, bilirubin binds site 3, and salicylate binds site 6. Site 4 is a metal binding site that was not considered in the present study because

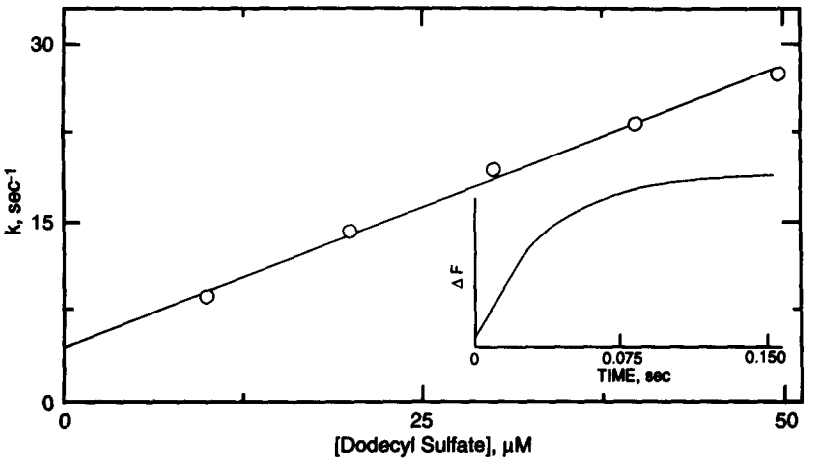

Fig. 7. Kinetics for the displacement of I from HSA·I by dodecyl sulfate. A typical time course for the fluorescence increase upon mixing the HSA·I complex (0.4 μM HSA and 1 μM I) with an equal volume of 100 μM dodecyl sulfate is presented in the inset. The pseudo first-order rate for this fluorescence change was linearly dependent on dodecyl sulfate concentration. The solid line was calculated from a fit of equation 3a to these data.

of the strong chelating properties of I. Site 5, which is a hemin binding site, was also not considered in the present study. The effect of these ligands on the rate constant for the binding of I to HSA was investigated to determine whether any of the binding regions defined by these ligands were involved in the binding of I to HSA. Any ligand that competed with I for the same binding site on HSA would decrease the apparent association rate constant for binding of I to HSA. The concentration of HSA (10 μM) was chosen to be in excess of the concentration of I (2.5 μM) in these experiments so that the binding reaction was first-order in the concentration of I. Furthermore, the potentially competing ligand was mixed with HSA prior to measuring the rate of binding of I to HSA to ensure that the competing ligand had time to equilibrate with HSA. The pseudo first-order rate constant for the reaction of I with HSA under these conditions was not greatly reduced (<50% in most cases) by any of the ligands tested (Table 1). Since the concentrations of these ligands were high relative to their respective high-affinity binding constants and there was little effect on the rate constant for the reaction of I with HSA, I was not binding to site 1, 2, 3, or 6.

Structural contributions to the binding of I to HSA

In contrast to the large changes in the fluorescence of HSA associated with the binding of I, 5 μM II did not change the fluorescence of 0.2 μM HSA. However, the slight increase ($\Delta\varepsilon_{345} = 4.3\ mM^{-1}\ cm^{-1}$) in the absorbance of II at 345 nm was used to monitor the titration of II by HSA. The dissociation constant of II for HSA was estimated to be 340 ± 160 μM by titrating 10 μM II with HSA (0–500 μM). The large errors in this determination were the result of the small absorbance change and the high concentrations of HSA needed for the titration. Nonetheless, this result suggested that the 2-(chloroanilino)thiocarbonyl moiety (IV) (see Structure 2) was essential for high-affinity binding of I to HSA.

The potential contributions of the 2-(chloroanilino)thiocarbonyl and the 2-acetylpyridine thiocarbonohydrazyl moieties, the two domains of I, to the overall binding energy of I for HSA were estimated by determining the dissociation constants of III and IV for HSA. The binding of III to HSA was monitored by the increase in absorbance at 350 nm that occurred upon binding to HSA. Because this absorbance change was observed with I, II, and III, it resulted from the 2-acetylpyridine thiocarbonohydrazyl moiety of these compounds. The absorbance maximum for III was at 310 nm; the extinction coefficient was $25\ mM^{-1}\ cm^{-1}$. These spectral parameters were similar to those for I and II. The dissociation constant of III for HSA was 200 ± 50 μM. The relatively large error associated with this determination resulted from the small absorbance change and the high concentrations of HSA used for the titration.

The binding of IV to HSA was monitored by its quenching of HSA fluorescence. The absorbance maximum for IV was at 240 nm and the extinction coefficient was $8\ mM^{-1}\ cm^{-1}$. IV did not absorb at wavelengths greater than 280 nm. Thus, the quenching of HSA fluorescence by I was the result of the chloroanilino moiety. When the titration of 260 nM HSA by IV was monitored spectrofluorometrically with an excitation wavelength of 300 nm, which excited only tryptophan, and an emission wavelength of 340 nm, the dissociation constant was 53 ± 9 μM; 42% of the protein fluorescence was quenched. A similar titration of 65 nM HSA by IV that was monitored with an excitation wavelength of 280 nm, which excited tryptophan and tyrosine, yielded a dissociation

Table 1. Effect of ligands on the pseudo first-order rate constants for the binding of 2.5 μM I to excess HSA (10 μM) at pH 7*

Ligand	K_d† (μM)	k‡ (sec^{-1})	Amplitude‡ ($\Delta A_{370} \times 10^3$)
No addition	NA§	360 ± 20	8.3 ± 0.2
		49 ± 4	2 ± 0.2
Warfarin (100 μM)	5	160 ± 4	14.4 ± 0.1
		38 ± 2	5.6 ± 0.1
Octanoate (300 μM)	30	250 ± 6	7.6 ± 0.1
		20 ± 2	2.3 ± 0.1
Dodecyl sulfate (50 μM)	<1	270 ± 10	6.4 ± 0.1
		20 ± 2	2.3 ± 0.1
Bilirubin (15 μM)	0.01	150 ± 5	14.4 ± 0.1
		23 ± 2	7.2 ± 0.1
Salicylate (100 μM)	10	230 ± 6	8.6 ± 0.1
		20 ± 1	6.6 ± 0.1
Ibuprofen (40 μM)	0.4	250 ± 6	8.5 ± 0.1
		19 ± 2	3.4 ± 0.1

* HSA (20 μM) was premixed with twice the indicated concentration of ligand in the standard buffer. This solution was then mixed with an equal volume of 5 μM I on the stopped-flow spectrophotometer and the time course for binding was monitored at 370 nm.

† The literature values for the dissociation constants of the competing ligands are given [8] to demonstrate that the concentration of competing ligand is many times its dissociation constant. Consequently, the high-affinity binding sites for these ligands were occupied prior to initiation of the reaction with I.

‡ Binding was biphasic. The pseudo first-order rate constant and amplitude for the early phase of the reaction are reported on the upper line of the entry, and the values for the late phase of the reaction are reported on the lower line of the entry. The reported kinetic constants were calculated from an average of four time courses that each contained 400 data points. The reported errors for the fitted parameters were the square root of the variance calculated from the nonlinear fitting routine.

§ Not applicable.

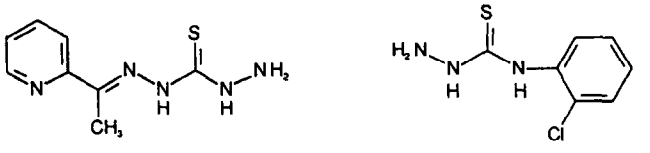

III IV

Structure 2.

constant of 41 ± 6 μM and 36% quenching of the enzyme fluorescence. Thus, similar results were obtained for titration of HSA by IV when binding was monitored by quenching of tryptophan fluorescence (excitation wavelength of 300 nm) or by tyrosine and tryptophan fluorescence (excitation wavelength of 280 nm). The pK_a values for I, II, III, and IV were determined by spectrometric titration to be 7.0 ± 0.1, 8.3 ± 0.1, 10.8 ± 0.1 and 11.1 ± 0.1, respectively.

If the binding energies for the domains of I characterized by III and IV were effectively used for binding of I to HSA, the dissociation constant for I could be calculated from the free energies for the binding of III (350 μM) and IV (45 μM). The dissociation constant calculated by this method was 0.020 μM, which was comparable to the measured high-affinity dissociation constant of HSA for I (0.11 μM).

Distance between I and tryptophan in HSA·I

The binding of I to HSA (Lot 1) was biphasic when the titration was monitored spectrofluorometrically with an excitation wavelength of 280 nm (Fig. 3), which excited both tyrosine and tryptophan. HSA fluorescence was quenched by 36% in the early phase of the titration and 39% in the later phase of the titration. An independent titration with HSA (Lot 2) yielded 48% quenching in the early phase (K_d = 230 ± 20 nM) and 32% quenching in the late phase of the titration (K_d = 2.2 ± 0.5 μM). When the excitation wavelength was increased to 295 nm,

there was 12% quenching in the early phase and 82% quenching in the late phase of the titration. When the excitation wavelength was increased to 300 nm such that only tryptophan was excited, the titration was monophasic with 75% quenching and a K_d of 1.7 ± 0.06 μM. thus, binding of I to HSA at the high-affinity site appeared to affect tyrosine fluorescence greater than tryptophan fluorescence.

The titration data determined with an excitation wavelength of 300 nm were used for the calculation of the distance between tryptophan and I. This site was the region of HSA that bound I with a dissociation constant of around 2 μM and was not the site with the highest affinity. Under these conditions there was 75% quenching of the protein fluorescence. However, IV, which had a spectral overlap integral with HSA that was essentially zero (i.e. the extinction coefficient for IV was zero at wavelengths greater than 280 nm), quenched the fluorescence of HSA by 42%. Since the quenching of HSA fluorescence by IV must result from a conformational change and not the Förster dipole-dipole excitation transfer mechanism, the relative fluorescence yield of HSA·I in the absence of fluorescence energy transfer (Q_0) was taken to be 58% (100 − 42%). The fluorescence of HSA·I was 25% of HSA (Q_t). The efficiency for quenching (E) was calculated from equation 6 to be 0.57. The spectral overlap integral (J) between the absorption spectrum of I and the emission spectrum of HSA (excitation wavelength 300 nm, data not shown) was $2.6 \times 10^{-14}\,M^{-1}\,cm^3$ (equation 5). R_0 for I and HSA was calculated from equation 4 to be 32 Å. Thus, the distance between tryptophan and the binding region of HSA·I with a dissociation constant of 2 μM was estimated from equation 7 to be 31 Å.

DISCUSSION

The binding of I to HSA caused a quenching of protein fluorescence and an increase in the absorbance at 370 nm. These spectral changes were used to monitor the binding of I to HSA. The time courses for binding of I to HSA were biphasic. These time courses could result from either multiple binding sites for I on HSA (parallel binding mechanism) or a site that formed an initial complex that sequentially rearranged to a complex with different spectral properties (consecutive binding mechanism). If the data of Fig. 4B were interpreted in terms of a consecutive binding mechanism, the K_d for formation of the initial complex should be greater than that for formation of the subsequent complex. Experimentally, the K_d for the initial complex was 0.8 μM and the K_d for the second phase of the reaction was 5 μM (Fig. 4B). Thus, the biphasic nature of the binding reaction probably resulted from multiple binding regions on HSA for I. This conclusion was consistent with spectral titration data that indicated at least three binding regions for I on HSA (Fig. 2).

The time courses for the binding of warfarin and bilirubin to HSA are also multiphasic [23–27]. The late phase of the time course for the binding of warfarin to HSA is attributed to a conformation change of the warfarin·HSA complex [25]. This consecutive binding mechanism contrasts with the parallel binding mechanism presented herein for the binding of I to HSA. A complication to the interpretation of any of these kinetic data is the observation that the binding isotherms for decanoate could not be fitted to the stoichiometric binding equation, which assumes that there is one albumin component with several binding sites [10]. A binding equation derived for a model that assumed two albumin components, each with a high-affinity and a low-affinity site for decanoate [10], fitted the data best. Even though the stoichiometric binding equation (equation 1) fitted the binding data for I and HSA within the experimental limits of the data, the possibility that there were two albumin components with different sets of binding affinity for I was not eliminated. In summary, the multiphasic time courses for the fluorescence changes upon binding of I to HSA were consistent with several binding sites in these albumin preparations and were not consistent with one binding site for I that isomerized after formation of the initial complex.

The rate of clearance of free drug from blood is dependent on the affinity of the drug for HSA [7]. However, the rate of drug clearance is not only dependent on the ratio of the association and dissociation rate constants of the drug for HSA, but is also dependent on the magnitude of the dissociation rate constant. Thus, if the half-time for dissociation of a ligand from HSA approaches the transit time of blood through an organ (1–10 sec [25]), the rate of clearance of the ligand by an organ of high elimination capacity could be limited by the dissociation rate constant and not the dissociation constant of the drug for HSA. Because the dissociation rate constant of I from HSA·I had a half-life of 0.10 sec, the clearance of I by organs with high elimination capacity would probably not be limited by this dissociation rate constant. However, the clearance of I would probably be limited by the low concentration of free I in serum, resulting from the high affinity of HSA for I. Since the concentration of HSA in serum is around 700 μM [29] and the dissociation constant of I for HSA was 0.11 μM, the concentration of free I in serum that contained 10 μM I is around 2 nM. If the concentration of free I in serum was not elevated significantly by displacement of I from HSA·I by fatty acids or other blood components, the rate of clearance of I from blood would probably be limited by the low concentration of I in serum.

The binding regions on HSA have been functionally classified into numerous domains by competition experiments with different ligands. Kragh-Hansen [8] proposed six major binding regions in addition to numerous other regions. This complexity suggests that HSA has great adaptability and plasticity in the formation of sites through conformation changes induced by ligand binding [29, 30]. Nonetheless, if a ligand bound to the same region as I, the association rate constant of I determined in the presence of the competing ligand should decrease. The association rate constant of HSA for I was decreased only slightly by bilirubin, warfarin, salicylate, ibuprofen, octanoate, and dodecyl sulfate at concentrations that were many times the respective dissociation constant

for these potentially competing ligands (Table 1). Thus, I was not binding directly to regions on HSA that bound any of these ligands, and the small effects that these ligands had on the association rate constants could be attributed to allosteric effects.

Octanoate and dodecyl sulfate both caused the dissociation of HSA·I. The binding properties of HSA for ligands such as a spin-labeled anionic ligand or warfarin are affected allosterically by fatty acids [31–34]. These results and those of Fig. 6 suggested that dissociation of I from HSA·I in the presence of octanoate or dodecyl sulfate resulted from an allosteric effect and not direct displacement of I from HSA·I. This would be analogous to the indirect displacement of ceftriaxone from HSA by diazepam [35].

When HSA was monitored spectrofluorometrically with an excitation wavelength of 280 nm, which excited both tyrosyl and tryptophanyl residues, the fluorescence of HSA decreased biphasically with increasing concentrations of I. A model with two dissociation constants with values of 0.11 and 5 μM were fitted to these data (Fig. 3). When the titration was monitored by the absorbance changes at 370 nm, the stoichiometric binding equation fitted the data with similar dissociation constants (Fig. 2). However, when the titration of HSA was monitored spectrofluorometrically with an excitation wavelength of 300 nm, which excited only tryptophanyl residues, the titration curve was described by a single binding function with a dissociation constant of 1.7 μM. The difference between the titration data obtained with an excitation wavelength of 280 nm versus 300 nm could be explained if the binding of I at the high-affinity region of HSA interfered with the transfer of energy from tyrosine to tryptophan but had little effect on the fluorescence of tryptophan. This phenomenon was not investigated further. The distance between the single tryptophan in HSA and I bound to the site with a dissociation constant of 2 μM was estimated to be 31 Å. Since the spectral overlap integral between I and the tryptophan fluorescence of HSA was relatively large, it was not apparent why I did not quench the fluorescence of HSA when I was bound to the high-affinity site. Possibly, the orientation factor for energy transfer between tryptophan and I bound to the high-affinity site was small.

The present study has investigated the binding of I to HSA in the absence of acyclovir. Because of the low affinity of serum proteins for acyclovir [36] and the large extinction coefficient of acyclovir at 280 nm, a study of the effect of acyclovir on the binding of I to HSA by the spectroscopic techniques used herein was not possible. Nonetheless, the low affinity of acyclovir for serum proteins made it unlikely that the affinity of I for HSA was changed by acyclovir. The combination of I (BW348U87) and acyclovir is currently being developed as a topical therapy for cutaneous herpes infection. II was initially considered for this therapy, but oral dosing of rats with II resulted in minor hematological toxicity. Even though these analogues are not being considered for oral dosing, I was chosen over II because it was hematologically nontoxic. The toxicity of bilirubin is reduced by binding to HSA [8, 9]. By analogy, the differential hematological toxicity of I and II could be related to the differential affinity of I and II for HSA. The results presented herein demonstrated that HSA bound I 3000-fold tighter than II. Thus, the tight binding of I to HSA (0.11 μM) versus the weak binding of II (340 μM) could reduce the toxicity of I relative to that of II in the same way that the toxicity of bilirubin is reduced by binding to HSA.

Acknowledgements—The author acknowledges Dr. John Reardon, Dr. Eric Furfine, and Dr. Thomas Spector for helpful discussions during the course of this work.

REFERENCES

1. Spector T, Lobe DC, Ellis MN, Blumenkopf TA and Szczech GM, Inactivators of herpes simplex virus ribonucleotide reductase: Hematological profiles and *in vitro* potentiation of the antiviral activity of acyclovir. *Antimicrob Agents Chemother* **36**: 982–988, 1992.
2. Spector T, Harrington JA, Morrison RW Jr, Lambe CU, Nelson DJ, Averett DR, Biron K and Furman PA, 2-Acetylpyridine 5-[(dimethylamino)thiocarbonyl] thiocarbonohydrazone (A1110U), a potent inactivator of ribonucleotide reductases of herpes simplex and varicella-zoster viruses and a potentiator of acyclovir. *Proc Natl Acad Sci USA* **86**: 1051–1055, 1989.
3. Spector T, Harrington JA and Porter DJT, Herpes and human ribonucleotide reductases. Inhibition by 2-acetylpyridine 5-[(2-chloroanilino)-thiocarbonyl]-thiocarbonohydrazone (348U87). *Biochem Pharmacol* **42**: 91–96, 1991.
4. Porter DJT, Harrington JA and Spector T, Herpes simplex type 1 ribonucleotide reductase: Selective and synergistic inactivation by A1110U and its iron complex. *Biochem Pharmacol* **39**: 639–646, 1990.
5. Ellis MN, Lobe DC and Spector T, Synergistic therapy by acyclovir and A1110U for mice orofacially infected with herpes simplex virus. *Antimicrob Agents Chemother* **33**: 1691–1696, 1989.
6. Lobe DC, Spector T and Ellis MN, Synergistic topical therapy by acyclovir and A1110U for herpes simplex virus induced zosteriform rash in mice. *Antiviral Res* **15**: 87–100, 1991.
7. Vallner JJ, Binding of drugs by albumin and plasma proteins. *J Pharm Sci* **66**: 447–465, 1977.
8. Kragh-Hensen U, Molecular aspects of ligand binding to serum albumin. *Pharmacol Rev* **33**: 17–53, 1981.
9. Ivarsen PR and Brodersen R, Displacement of bilirubin from adult and newborn serum albumin by a drug and fatty acid. *Dev Pharmacol Ther* **12**: 19–29, 1989.
10. Honoré B and Brodersen R, Detection of carrier heterogeneity by rate of ligand dialysis: Medium-chain fatty acid interaction with human serum albumin and competition with chloride. *Anal Biochem* **171**: 55–66, 1988.
11. Blumenkopf TA, Harrington JA, Koble CS, Bankston DD, Morrison RW Jr, Bigham EC, Styles VI and Spector T, 2-Acetylpyridine thiocarbonohydrazones. Potent inactivators of herpes simplex virus ribonucleotide reductase. *J Med Chem* **35**: 2306–2314, 1992.
12. Koh SM and Means GE, Characterization of a small apolar anion binding site of human serum albumin. *Arch Biochem Biophys* **192**: 73–79, 1979.
13. Reed RG, Kinetics of bilirubin binding to bovine serum albumin and the effect of palmitate. *J Biol Chem* **252**: 7483–7487, 1977.
14. Klotz IM and Hunston DL, Protein affinities for small molecules: Conceptions and misconceptions. *Arch Biochem Biophys* **193**: 314–328, 1979.

15. Fletcher JE, Spector AA and Ashbrook JD, Analysis of macromolecule-ligand binding by determination of stepwise equilibrium constants. *Biochemistry* **9**: 4580–4587, 1970.
16. Bevington PR, *Data Reduction and Error Analysis for the Physical Sciences*, pp. 204–246. McGraw-Hill, New York, 1969.
17. Berde CB, Hudson BS, Simoni RD and Sklar LA, Human serum albumin: Spectroscopic studies of binding and proximity relationships for fatty acids and bilirubin. *J Biol Chem* **254**: 391–400, 1979.
18. Stryer L, Fluorescence energy transfer as a spectroscopic ruler. *Annu Rev Biochem* **47**: 819–846, 1978.
19. Reinard T and Jacobsen H-J, An inexpensive small volume equilibrium dialysis system for protein–ligand binding assays. *Anal Biochem* **176**: 157–160, 1989.
20. Fersht A, *Enzyme Structure and Mechanism*, p. 140. W. H. Freeman, New York, 1985.
21. Steinhardt J, Krijn J and Leidy JG, Differences between bovine and human serum albumins: Binding isotherms, optical rotatory dispersion, viscosity, hydrogen ion titration and fluorescence effects. *Biochemistry* **10**: 4005–4015, 1977.
22. Kragh-Hensen U, Octanoate binding to the indole- and benzodiazepine-binding region of human serum albumin. *Biochem J* **273**: 641–644, 1991.
23. Rietbrock N and Lassmann A, Stopped-flow studies on drug–protein binding. I. Kinetics of warfarin binding to human serum albumin. *Naunyn Schmiedebergs Arch Pharmacol* **313**: 269–274, 1980.
24. Rietbrock N, Menke G, Reuter G, Lassmann A and Schmeidl R, Influence of palmitate and oleate on the binding of warfarin to human serum albumin: Stopped-flow studies. *J Clin Chem Clin Biochem* **23**: 719–723, 1985.
25. Lassmann A and Rietbrock N, Insights into drug protein binding obtained by stopped-flow measurements. In: *Aggregation Processes in Solution* (Eds. Wyn-Jones E and Gormally J), pp. 383–409. Elsevier, Amsterdam, 1982.
26. Wilting J, van der Giesen WF, Janssen LHM, Weidemann MM, Otagri M and Perrin JH, The effect of albumin conformation on the binding of warfarin to human serum albumin. *J Biol Chem* **255**: 3032–3037, 1980.
27. Jacobsen J and Brodersen R, Albumin–bilirubin binding mechanism. Kinetic and spectroscopic studies of binding of bilirubin and xanthobilirubic acid to human serum albumin. *J Biol Chem* **258**: 6319–6326, 1983.
28. Diem K and Lentner C (Eds.), *Scientific Tables*, 7th Edn, p. 582. Geigy Pharmaceuticals, Ardsley, NY, 1970.
29. Spector AA, Fatty acid binding to plasma albumin. *J Lipid Res* **16**: 165–179, 1975.
30. Brodersen R, Honoré B and Larsen FG, Serum albumin—A non-saturable carrier. *Acta Pharmacol Toxicol* **54**: 129–133, 1984.
31. Soltys BJ and Hsia JC, Fatty acid enhancement of human serum albumin binding properties: A spin label study. *J Biol Chem* **252**: 4043–4048, 1977.
32. Hsia JC and Kwan NH, Human serum albumin: Binding specificity and allosteric effect of parinarate and stearate: A dianionic spin label study. *J Biol Chem* **256**: 2242–2244, 1981.
33. Chakrabarti SK, Cooperativity of warfarin binding with human serum albumin induced by free fatty acid anion. *Biochem Pharmacol* **27**: 739–743, 1978.
34. Droge JHM, Janssen LHM and Wilting J, Evidence for the fatty acid-induced heterogeneity of the N and B conformations of human serum albumin. *Biochem Pharmacol* **34**: 3299–3304, 1985.
35. McNamara PJ, Trueb V and Stoeckel K, Ceftriaxone binding to human serum albumin: Indirect displacement of probenecid and diazepam. *Biochem Pharmacol* **40**: 1247–1253, 1990.
36. de Miranda P, Krasny HC, Page DA and Elion GB, The disposition of acyclovir in different species. *J Pharmacol Exp Ther* **219**: 309–315, 1981.